



Structural, Morphological and Optical Properties of ZnS : Mn Doped Polyaniline Nanocomposites

S. Jayasudha¹, L. Priya^{2*}, K. T. Vasudevan³

¹Department of Physics, CPGS, Jain University, Bangalore, KA, India

²Department of Physics, LRG Govt. Arts College for Women, Tirupur, TN, India

³Department of Physics, T. John College, Bangalore, KA, India

Received: 18.07.2017 Accepted: 02.08.2017 Published: 30-09-2017

*svlpriya1@gmail.com

ABSTRACT

Nanocomposites of conducting polyaniline with ZnS:Mn nanoparticle (PAni/ZnS:Mn) have been synthesised by chemical co-precipitation method. The weight percentage of ZnS:Mn varied from 1 to 28%. PAni/ZnS:Mn nanocomposites has been synthesised by adding the ZnS:Mn precipitate in to the prepared Polyaniline solution. The Structural and morphological properties have been studied by X-ray diffraction and Field Emission scanning electron microscopy. Optical characterization has been done by UV-Vis and Photoluminescence. From XRD pattern prominent peak of PAni as well as ZnS:Mn are observed. Using Scherrer formula the particle size of ZnS: Mn was also calculated. FESEM image shows uniform distribution of ZnS:Mn on PAni matrix. UV-Vis graph of PAni/ZnS:Mn nanocomposites shows three peaks in common at ~250 nm, and broad peaks at ~300 – 350 nm and ~400 – 450 nm. From UV-Vis graph it is observed that the composites peak got blue shifted compared to ZnS:Mn. Photoluminescence emission of PAni/ZnS:Mn shows 5 peaks at ~273 nm, ~308 nm, ~400 nm, ~464 nm and ~484 nm. From the PL spectra it is also observed that as the ZnS:Mn concentration increases in the composites there is a shift of peak position compared to ZnS:Mn.

Keywords: Diamine; Piperonal; Tetrazole.

1. INTRODUCTION

Conducting polymers and composites are one of the major areas of experimental research ever due to the possibility to control electrical conductivity of these films from insulating to metallic by doping. A number of metal and metal oxide particles have been encapsulated into the conductive polymer to form nanocomposites. The incorporation of metal nanoparticles acts as a conductive junction between PAni resulting in an increase electrical properties of the polyaniline composites. These properties are extremely sensitive to small changes in content, size and shape of the metal nanoparticles incorporated.

ZnS nanoparticles added with transition metal ions and rare earth ions have distinct optical properties related to traditional bulk materials. These nanocomposites widely used as photoluminescence and electroluminescence devices. Luminescence of rare-earth doped systems mainly indicates the features of the dopant. Doped ZnS semiconductor materials have extensive range of application in phosphors, light emitting displays, and optical sensors (WQ Peng *et al.* 2005). Mn²⁺ ions occupy cation position in ZnS lattice. The impurities of manganese isomorphically replace zinc in the lattice. The degree of homogeneity of Mn²⁺ ions is essential for high efficient luminescence (G. Murugadoss

et al. 2009). ZnS doped with Mn²⁺ nanomaterials are having high quantum efficiency and luminous intensity. Among the synthesis techniques chemical co-precipitation is most popular due to its advantages like it is simple to synthesize.

In this work, PAni/ZnS:Mn were prepared by a chemical co-precipitation method. Structural and morphological properties have been studied by X-ray diffraction and Field Emission scanning electron microscopy. Optical characterization has been done by UV-Vis and Photoluminescence.

2. EXPERIMENTAL TECHNIQUE

Analytical grade Aniline monomer, Hydrochloric acid and Ammonium persulphate were purchased from Qualigens, and silver nitrate is purchased from Merck chemicals.

Aniline and Ammonium persulphate are prepared in 1:1.2 molar ratios in 3M HCl. Ammonium persulphate solution was added drop by drop to the prepared aniline solution over a period of 30 min with continuous stirring. A dark green colour was seen indicating the formation of polyaniline. Polymerized sample was purified by dialyzing against distilled water and is dried to form films at room temperature.

Freshly prepared aqueous solutions of the chemicals were used for the synthesis of nanoparticles. These particles were prepared at room temperature by dropping simultaneously 100ml solution of 0.4M of Zinc Sulphate, 100ml of 0.1M solution of Manganese Sulphate and 100ml of 0.5M solution of Sodium Sulphide into 250ml of distilled water containing 100ml of 0.1M solution of EDTA which was vigorously stirred using magnetic stirrer. The role of EDTA is to stabilize the particles against aggregation. The prepared reaction mixture was kept for stirring for two hours at constant rate of stirring after which the mixture was precipitated. The precipitated mixture was then separated from the reaction mixture, washed twice with distilled water to remove the impurities and the smell. The wet precipitate was dried and thoroughly grinded.

For the preparation of PANi/ ZnS:Mn nanocomposite, first ZnS:Mn nanoparticles were prepared. The precipitate was washed and dried. Then PANi was prepared and after 2 hours of stirring, ZnS:Mn precipitate was mixed in the PANi solution. It was stirred continuously for 24 hrs. Dialysis was carried out for 48 hours against double distilled water and the dialyzed solution was kept for drying. By varying the weight concentrations various compositions were prepared.

3. RESULTS & DISCUSSIONS

3.1 XRD

Fig. 1 illustrate the XRD pattern of PANi, ZnS:Mn and PANi/ZnS:Mn of various concentrations. XRD pattern of ZnS:Mn shows 4 peaks at 28.51° , 47.6° , 56.3° , 76.76° . Intense broad peak at 28.51° corresponding to (110) plane of ZnS:Mn indicates the formation of nanostructure (Jyothi P. Borah *et al.* 2008). XRD pattern also shows three prominent peaks at 47.8° and 56.3° and 76.76° correspond to (220), (311) and (331) plane of zinc blend structure. There is an obvious broadening of the XRD pattern which indicates the formation of nano sized ZnS:Mn.

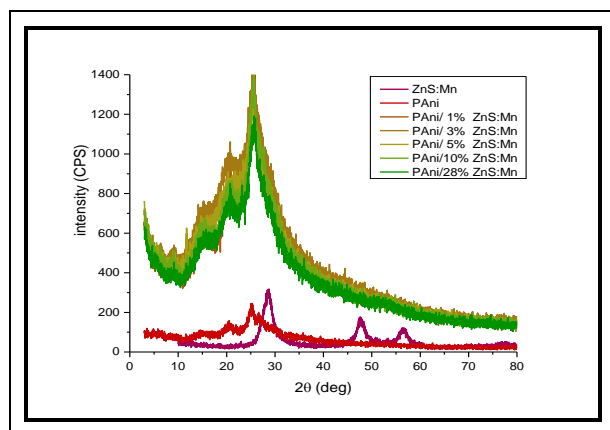


Fig. 1: XRD of PANi, ZnS : Mn and its nanocomposites.

The XRD pattern of nanocomposites shows prominent peak at 25.42° for all the concentrations and also both prominent peak of PANi and ZnS:Mn are seen. The peak at 28.51° is shifted to lower 2θ value at 25.42° in nanocomposites. The shift of peak to the lower 2θ may be due to the variation of ionic radius of Zn and Mn and Mn^{2+} ions occupying ZnS sites.

As the concentration of ZnS:Mn increased in the nanocomposites, the peak intensity is found to increase till 10%. When the concentration of ZnS:Mn is further increased the peak intensity got decreased indicating disorganization in the structure. The decrease in peak intensity can also be attributed to increase of new nucleating centres. Broadening of the peak confirms the reduction of particle size.

The average particle size of the crystallites of each sample were determined from the full-width at half maxima (FWHM) of the XRD peaks by using the Scherrer formula. The particle size of ZnS:Mn is found to be ~ 6 nm.

3.2 FESEM

FESEM micrograph of PANi, ZnS : Mn and its nanocomposites are presented in fig. 2. It is observed that ZnS:Mn particles are homogeneously dispersed in PANi matrix within nano range and it is almost spherical in shape. As it is evenly distributed, ZnS:Mn are well interconnected which assist in the ionic conduction. The FESEM images help us draw a conclusion that the doping of ZnS:Mn has a strong effect on the morphology of PANi. It was observed that PANi prevented the agglomeration of ZnS:Mn to a certain level, this helps in easy transfer of electrons from PANi to ZnS:Mn. Some small particles are found which play an important role in the “size quantization effect”.

3.3 UV-Vis Analysis

Fig. 3 shows the UV-Vis analysis of PANi, ZnS:Mn, and PANi/ZnS:Mn. The UV-Visible absorption spectra of these samples have been recorded in the range of 190 to 1100 nm. The transitions occurred in range 280 - 840 nm is attributed to polaron/bipolaron transition of doped PANi. PANi shows three peaks at ~ 198 nm and ~ 324 nm and a broad peak around $\sim 600 - 800$ nm. ZnS:Mn shows three peaks at ~ 373 nm, ~ 905 nm and ~ 968 nm

PANi/ZnS:Mn nanocomposites shows three peaks in common at ~ 250 nm, and a broad peak at $\sim 300 - 350$ nm and $\sim 400 - 450$ nm. There are some additional peak found at ~ 550 nm, ~ 840 nm and ~ 920 nm. The variation in peak position indicates change of the particle size.

As observed in the figure, the samples exhibits an excitonic peak around 250 nm for

PAni/ZnS:Mnnanocomposites. The absorption peaks of PAni/ZnS:Mn are considerably blue shifted compared to ZnS:Mn. This absorption edge indicates increase in effective bands of the doped PAni samples.

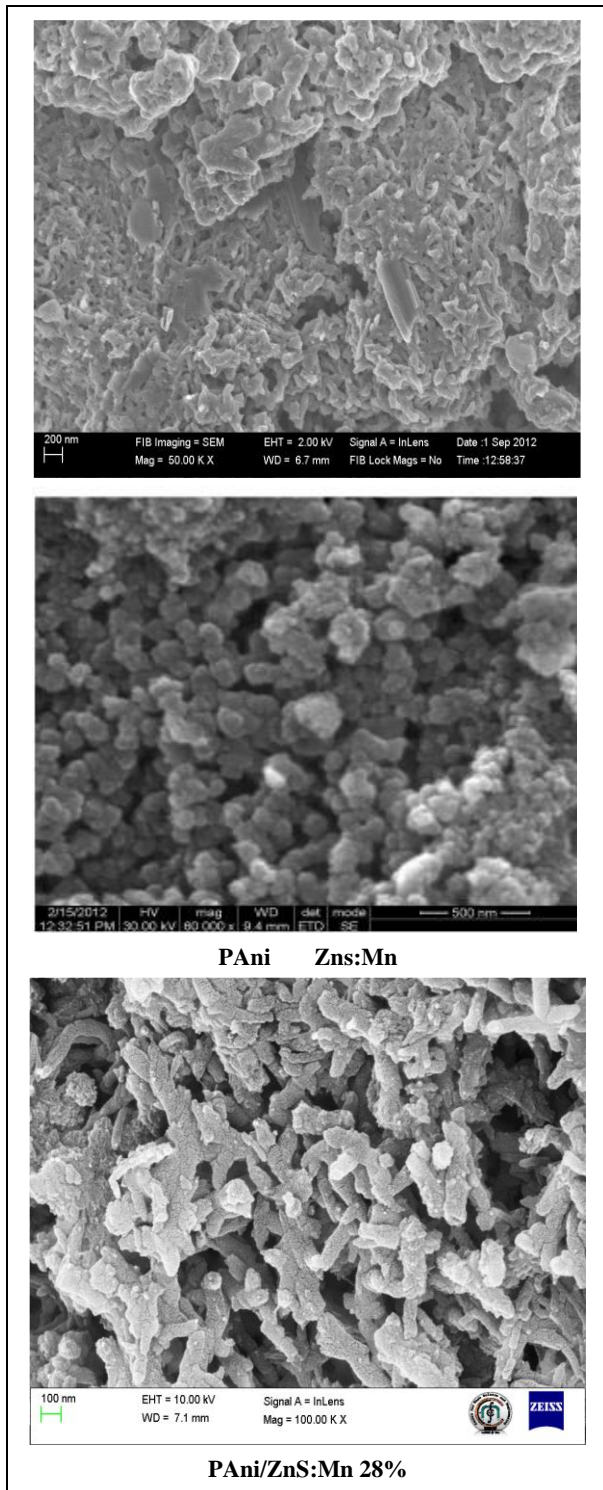


Fig. 2: FESEM image of PANi, ZnS and PANi/ZnS:Mn.

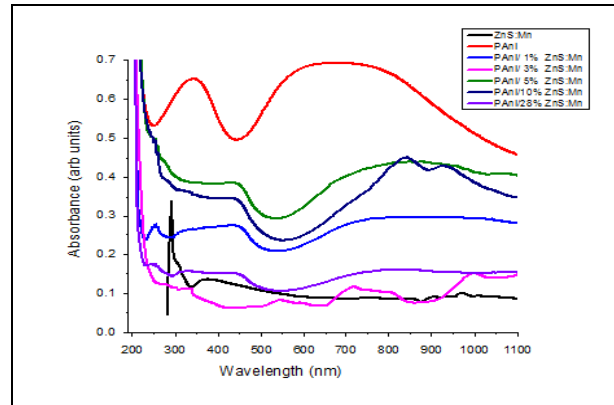


Fig. 3: UV-Vis Analysis of PANi, ZnS and PANi/ZnS:Mn.

The characteristic absorption peaks appear in the range ~300 – 350 nm and this peak position reflects the band gap of the synthesized particle. As the peak at ~300 – 350 nm shows a broad absorption for some concentration, means that there is a transition from valence band to conduction band, and in some concentration the same peak shows a weak absorption, this weak absorption arises from transition involving extrinsic state like defect states or impurities (Vidya et al. 2014, 2015).

The region between ~400 – 450 nm, belongs to the energy absorbed by ZnS:Mn. This peak is also attributed to the doping level of PANi (Yu-Feng Lin et al. 2006). Peak at ~550 nm belongs to enhancement green emission that is observed in 1% and 3% (Pin-Chun Shen et al. 2014). The absorption at ~550 nm of 1% and 3% of nanocomposites are assigned to the n - π* transition of protonated form of PANi.

3.4 Photoluminescence Analysis

Photoluminescence (PL) of the ZnS:Mn, PANi and nanocomposites samples are measured at room temperature. The PL spectrum of PANi and nanocomposites with ZnS:Mn is inset as shown in figure 4. ZnS:Mn and nanocomposites are excited with a wavelength of 275 nm, whereas PANi is excited with a wavelength of 320 nm. PL spectrum of ZnS:Mn contains 7 peaks, among the 7 peaks one peak lies in UV region and the remaining 6 peaks lies in the visible region of the spectrum.

Amongst all the PL peaks, UV emission peak at ~376 nm is due to the surface bound Mn²⁺ ion (Sana et al. 2012). Intense peak at ~404 nm is attributed to the sulphur vacancies; the peak at ~423 nm occurs due to self-trapping holes centres of ZnS. A blue emission peak at ~443 nm is related with the defect related emission of ZnS host.

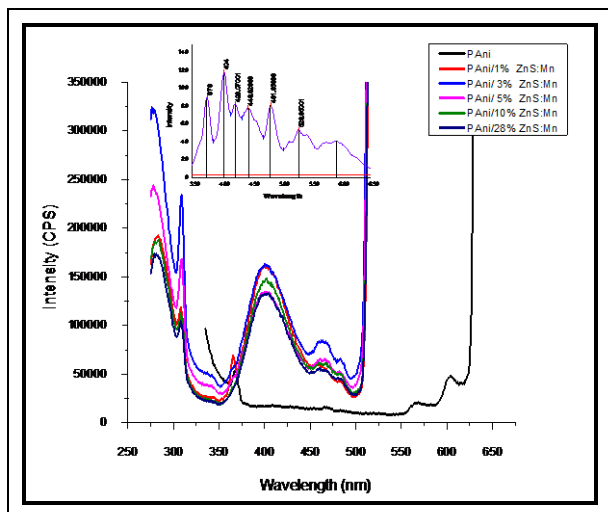


Fig. 4: PL analysis of PANi and PANi / ZnS : Mn nanocomposites with various wt% of ZnS:Mn in inset.

PL emission at ~ 481 nm is ascribed to the loose sulphur bonds at the interface of ZnS nanoparticles. A green emission at ~ 530 nm is assigned to the elemental sulphur particles on the surface of ZnS (A.K. Kole *et al.* 2012; Ye *et al.* 2004). PL peak at ~ 598 nm arises due to the excitation and subsequent de excitation of Mn^{2+} ions (R. Sharma *et al.* 2009). Photoluminescence emission of PANi/ZnS:Mn shows 5 peaks at ~ 273 nm, ~ 308 nm, ~ 400 nm, ~ 464 nm and ~ 484 nm. One of the reasons for PANi/ZnS:Mn to shift to lower wavelength is phonon coupling. This coupling strength is size dependent. Another reason might be when the exciton energy increases, the band gap increases and the absorption and emission spectra shifts to shorter wavelengths. This effect is called the quantum confinement effect.

4. CONCLUSION

PANi/ZnS:Mn nanocomposites were successfully synthesized by chemical co-precipitation method with different weight percentage of ZnS:Mn. The formations of ZnS:Mn nanoparticles in the nanocomposites were confirmed by XRD and FESEM. The optical characteristic was confirmed by photoluminescence and UV-Vis spectroscopy studies. The fibrillar structure of PANi and the linkage of these chains with ZnS:Mn nanoparticles could be the reason for the better conductivity in the nanocomposites. The XRD graph reveals the Zinc blende structure of ZnS:Mn. FESEM analysis showed the uniform dispersion of

spherical ZnS:Mn nanoparticles in the PANi matrix. UV-Vis analysis infer quantum confinement effect of ZnS:Mn. PL spectrum of ZnS:Mn shows 7 peaks in UV region and in the visible region of the spectrum.

FUNDING

This research received no specific grant from any funding agency in the public, commercial, or not-for-profit sectors.

CONFLICTS OF INTEREST

The authors declare that there is no conflict of interest.

COPYRIGHT

This article is an open access article distributed under the terms and conditions of the Creative Commons Attribution (CC-BY) license (<http://creativecommons.org/licenses/by/4.0/>).



REFERENCES

- Borah, J. P., et al., Structural and optical properties of ZnS nanoparticles, *Chalcogenide letters*, 5(9), 201–208 (2008).
- Kole, A. K. and Kumbhakar, P., Effect of manganese doping on the photoluminescence characteristics of chemically synthesized zinc sulfide nanoparticles, *Applied Nanoscience*, 2:15–23(2012). <https://doi.org/10.1007/s13204-011-0036-x>
- Murugadoss, G., et al., Synthesis and Characterization of Water-soluble ZnS: Mn^{2+} Nanocrystals, *Chalcogenide Letters*, 6:5: 197- 201(2009).
- Peng, W. Q., et al., Concentration effect of Mn^{2+} on the photoluminescence of ZnS:Mn nanocrystals, *Journal of Crystal Growth*, 279:3-4: 454 – 460(2005). <https://doi.org/10.1016/j.jcrysgro.2005.02.066>
- Pin-Chun Shen, Ming-Shiun Lin and Ching-Fuh Lin, Environmentally Benign Technology for Efficient Warm-White Light Emission, *Scientific Reports – Nature*, 4: 5307(2014). <https://doi.org/10.1038/srep05307>

- Sana, P., Lubna Hashmi and Malik, M. M., Luminescence and Morphological Kinetics of Functionalized ZnS Colloidal Nanocrystals, *International Scholarly Research Network*, 01–08(2012).
<https://doi.org/10.5402/2012/621908>
- Sharma, R., Chandra, B. P. and Bisen, D. P., Optical properties of ZnS:Mn nanoparticles prepared by chemical routs, *Chalcogenide Letters*, 6:8: 339 – 342(2009).
- Vidya, Y. S., Anantharaju, K. S., Nagabhushana, H., Sharma, S. D., Nagaswarupa, H. P., Prashantha, S. C., Shivakumara, C. and Danithkumar, Combustion synthesized tetragonal ZrO₂: Eu³⁺ nanophosphors: Structural and photoluminescence studies, *SpectrochimicaActa Part A: Molecular and Biomolecular Spectroscopy*, 135: 241– 251 (2015).
<https://doi.org/10.1016/j.saa.2014.06.151>
- Vidya, Y. S. and Lakshminarasappa, B. N., Synthesis, Characterization and Thermoluminescence Studies of LiNaSO₄: Eu³⁺ Nanophosphor, *Journal of Luminescence and Applications*, 1(2), 40-60(2014).
<https://doi.org/10.7726/jla.2014.1005>
- Ye, C., Xiaosheng Fang, Guanghai Li and Lide Zhang, Origin of the green photoluminescence from zinc sulfidenanobelts, *Applied Physics Letters*, 85: 3035 – 3037(2014).
<https://doi.org/10.1063/1.1807018>
- Yu-Feng Lin, Yen-Hwei Chang, Yee-Shin Chang, Bin-Siang Tsai and Yu-Chun Li, Photoluminescent properties of Ba₂ZnS₃:Mn phosphors, *Journal of Alloys and Compounds*, 421: 268 –272(2006).
<https://doi.org/10.1016/j.jallcom.2005.11.038>